Transition Metal Chemistry
https://doi.org/10.1007/s11243-018-0211-y

DNA binding, crystal structure, molecular docking studies and anticancer activity evaluation of a copper(II) complex

Ya-Xian Liu[1] · Hui-Wen Mo[1] · Zhen-Yu Lv[1] · Fang Shen[1] · Chun-Lian Zhang[1] · Yong-Yu Qi[1] · Zong-Wan Mao[2] · Xue-Yi Le[1]

Received: 13 November 2017 / Accepted: 26 January 2018

Abstract

A copper complex [Cu(HPBM)(L-Phe)(H_2O)]·ClO_4 **(1)** (HPBM = 5-methyl-2-(2′-pyridyl)benzimidazole, L-Phe = L-phenylalanine anion) was synthesized and characterized by elemental analysis, IR, ESI–MS, HR–ESI–MS, ESR spectroscopy, and by X-ray single-crystal analysis. The binding constant of the complex with calf thymus DNA (CT-DNA) was determined as 7.38 (± 0.57) × 10^4 M^{-1}. Further studies indicated that the complex interacts with CT-DNA through minor groove binding. The in vitro cytotoxic activities of both the free proligand and the complex against Eca-109, HeLa and A549 cancer cells and normal LO2 cells were evaluated by the MTT method. The IC_{50} values range from 5.7 ± 0.1 to 8.3 ± 0.6 μM. Free HPBM displays no cytotoxic activity against the selected cancer cells, with IC_{50} values more than 100 μM. Double staining analysis showed that the complex can induce apoptosis in Eca-109 cells. Comet assays demonstrated that the complex can damage DNA and cause apoptosis. The complex also induces an increase in intracellular reactive oxygen species and a reduction in mitochondrial membrane potential. The complex can also increase the intracellular Ca^{2+} level and induce release of cytochrome *c*. The cell cycle arrest was investigated by flow cytometry. The results demonstrate that the complex induces apoptosis in Eca-109 cells through DNA-binding and ROS-mediated mitochondrial dysfunctional pathways.

Introduction

One of the defining features of cancer is the rapid growth of abnormal cells beyond their usual boundaries, which can then invade adjoining parts of the body and spread to other organs [1]. In recent decades, the clinical success of cisplatin has provided an essential tool in cancer chemotherapy. However, many platinum drugs are also associated with side effects such as severe toxicity and drug resistance [2–4]. In an attempt to overcome such problems, a number of complexes based on other transition metals have been investigated [5–8]. In particular, the DNA interactions and anticancer activities of copper complexes have been extensively investigated [9–11]. As an essential trace element, copper is known to be involved in both metabolism and endogenous oxidative DNA damage associated with aging and cancer [12–14]. Recent research has shown that transition metal complexes of aromatic heterocyclic ligands can recognize nucleic acid and can be applied as DNA structure probes, footprinting agents, site-specific cleavage agents, DNA "molecular light switches" and anticancer drugs [15–18]. It is also known that biological activities can be higher when a small biomolecular ligand such as an amino acid, dipeptide and so on is incorporated into the compound [19–21]. In continuation of our interests in this field, we have synthesized and characterized a new aromatic heterocycle-based copper(II) complex with an amino acid co-ligand (Scheme 1). We have further explored the DNA binding and cleavage properties of the complex by electronic absorption titration, viscosity measurements, circular dichroism spectroscopy, cyclic voltammetry, DNA cleavage and molecular docking studies. In addition, the in vitro anticancer activity of the complex was investigated by MTT method, apoptosis, comet assay, reactive oxygen species

Electronic supplementary material The online version of this article (https://doi.org/10.1007/s11243-018-0211-y) contains supplementary material, which is available to authorized users.

✉ Xue-Yi Le
lexyfu@163.com

[1] Department of Applied Chemistry, South China Agricultural University, Guangzhou 510642, People's Republic of China

[2] MOE Key Laboratory of Bioinorganic and Synthetic Chemistry, School of Chemistry and Chemical Engineering, Sun Yat-Sen University, Guangzhou 510275, People's Republic of China

Published online: 01 February 2018

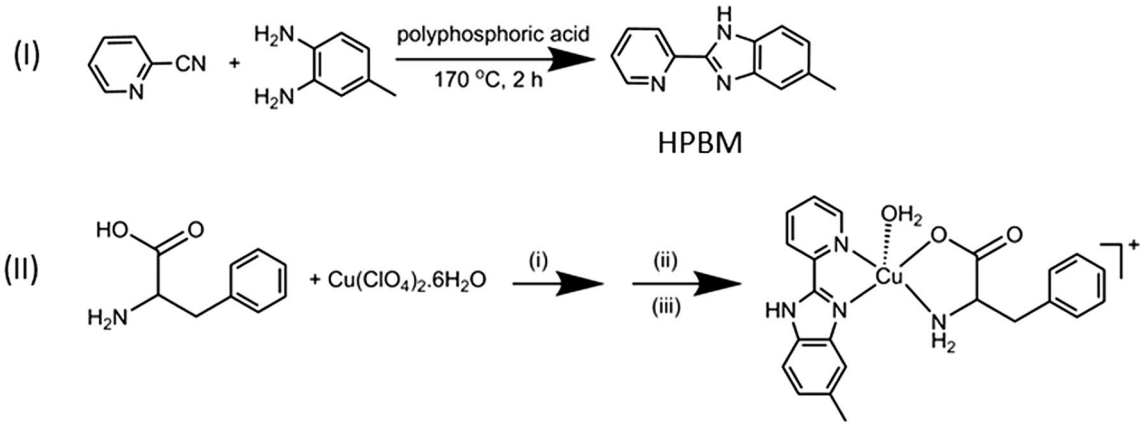

Scheme 1 The synthetic route of ligand HPBM and the Cu(II) complex. (i) H_2O, NaOH, 60 °C, 30 min, (ii) HPBM, (iii) MeOH, 60 °C, 2 h

assay, mitochondrial membrane potential, intracellular ROS levels, the release of cytochrome *c* and cell cycle arrest.

Experimental

Materials and instrumentation

The reagents and chemicals were obtained from commercial sources and used without further purification. L-Phenylalanine (L-Phe) was purchased from Aladdin. Calf thymus DNA (CT-DNA) (stored at 4 °C) was purchased from Sigma. pBR322 DNA was obtained from MBI Fermentas (Lithuania). 3-(4,5-Dimethylthiazol-2-yl)-2,5-diphenyltetrazolium bromide (MTT) and tetramethylethylenediamine (TEMED) were purchased from Sinopharm Chemical Reagent Co., Ltd. (Shanghai, China). Cancer cell lines consisting of HeLa (human cervical cancer cell line), A549 (human lung adenocarcinoma cell line), Eca-109 (human esophagus cancer cell line) and the normal human liver cell line LO2 were obtained from the Laboratory Animal Center of Sun Yat-Sen University (Guangzhou, China). Deionized water was used in all experiments. All experiments involving CT-DNA were performed in Tris–HCl buffer solution (pH 7.2) containing 5 mM Tris–HCl and 50 mM NaCl. Solutions of CT-DNA in Tris–HCl buffer gave a ratio of UV absorbance at 260 and 280 nm (A_{260}/A_{280}) of ca. 1.8–1.9, indicating that the DNA was sufficiently free of protein [22]. The concentration of DNA was determined by UV absorbance at 260 nm using the molar absorption coefficient of 6600 M^{-1} cm^{-1} [23]. DNA solutions were used after no more than 4 days.

Elemental analyses (CHN) were obtained with a Vario EL elemental analyzer (Elementar, Germany). ESI–MS spectra were measured using an API4000 triple quadrupole mass spectrometer (AB Sciex, USA). ESR spectra at liquid nitrogen temperature (90 K) were recorded in methanol solution on a Bruker EMX A300 spectrometer (Bruker, Germany) equipped with 100 kHz magnetic field modulation. IR spectra (KBr disks, 4000–400 cm^{-1}) were obtained with a VERTEX 70 FT-IR spectrometer (Bruker, Germany). UV–Vis spectra were recorded on a Pharmacia 2550 spectrophotometer (Shimadzu, Japan). Circular dichroism spectra were recorded using a Chirascan CD spectropolarimeter (Applied Photophysics Ltd., UK).

Synthesis of complex 1

To a solution of L-Phe (0.083 g, 0.50 mmol) in water (5 mL), plus NaOH (0.02 g, 0.50 mmol), was added a solution of $Cu(ClO_4)_2{\cdot}6H_2O$ (0.185 g, 0.50 mmol) dissolved in water (5 mL) with stirring. A solution of HPBM [24] (0.105 g, 0.50 mmol) in MeOH (20 mL) was then added dropwise, with stirring continued for 2 h at 50 °C. The resulting solution was filtered, and the filtrate was slowly evaporated at room temperature until a blue microcrystalline product was obtained. This was then recrystallized from MeOH to give X-ray quality single crystals. Yield: 70%. Anal calc for $C_{22}H_{23}N_4O_7ClCu$: C, 47.66; H, 4.15, N, 10.11%. Found: C, 47.62; H, 4.13; N, 10.07%. Λ_M/Ω^{-1} cm^2 mol^{-1}: 87.8. $\lambda_{max/nm}$, in MeOH (ε_{max}/dm^3 mol^{-1} cm^{-1}): 208 (49,936), 344 (19,017). IR (KBr, cm^{-1}): 3446m, 3321w, 3269w, 3138w, 1589s, 1454m, 1404s, 1120s, 1093s, 758m, 625m. ESI–MS (MeOH): m/z = 436 $[Cu(HPBM)(L\text{-}Phe)]^+$. HR-ESIMS m/z for $C_{22}H_{21}^{63}CuN_4O_2$ ($M + H^+$) calcd (found): 436.09605 (436.09464). ESR (MeOH): $g_{\|}$ = 2.276, $g_{\perp}$ = 2.044, A_{II} = 171.1 G.

Crystal structure determination and refinement

X-ray diffraction measurements were performed with a Bruker Smart CCD area detector in the range $4.33 < \theta < 75.33°$ with Cu K_α radiation (λ = 1.54178 Å)

at 293 K. Empirical absorption corrections were applied using the SADABS program [25]. The structure was determined using pattern methods, which yielded the positions of all non-hydrogen atoms. All the hydrogen atoms of the complex were placed in calculated positions with fixed isotropic thermal parameters and the structure factor calculations were included in the final stage of full-matrix least-squares refinement. All calculations were performed using the SHELXTL-97 suite of computer programs [26].

Crystallographic data (excluding structure factors) for the structures reported in this work have been deposited with the Cambridge Crystallographic Data Centre as supplementary publication no. CCDC-1560445. Copies of the data can be obtained free of charge on application via www.ccdc.cam.ac.uk/data_request/cif or e-mail (deposit@ccdc.cam.ac.uk).

Electronic absorption titrations

Absorption spectra titration was carried out with a fixed concentration of the Cu(II) complex (50 μM) while gradually increasing the concentration of DNA. To eliminate the impact of absorbance changes due to DNA, equal volumes of DNA were added to both the sample and reference cells. After addition of DNA to the metal complex, the resulting solutions were equilibrated for 5 min at room temperature. The absorption spectra were then recorded in the range of 200–500 nm. In order to quantitatively evaluate the DNA-binding affinity, the intrinsic binding constant K_b was determined using the Wolfe–Shimmer equation [27]:

$$[\mathrm{DNA}]/(\varepsilon_a - \varepsilon_f) = [\mathrm{DNA}]/(\varepsilon_a - \varepsilon_f) + 1/K_b(\varepsilon_b - \varepsilon_f) \quad (1)$$

where [DNA] is the concentration of DNA in the base pairs, ε_a, ε_f and ε_b correspond to the apparent extinction coefficient (A_{obsd}/[Cu]), the extinction coefficient of the free (unbound) and fully bound complex, respectively. From the plot of [DNA]/($\varepsilon_a - \varepsilon_f$) versus [DNA], the binding constant K_b was given by the ratio of the slope to the intercept.

Viscosity experiments

Viscosity experiments were performed using an Ubbelohde viscometer maintained at constant temperature (25.0 ± 0.1 °C) in a thermostatic water bath. The flow time was measured using a digital stopwatch. Each flow time was measured in triplicate, and an average flow time was calculated. The values of $(\eta/\eta_0)^{1/3}$, where η and η_0 represent the viscosity of CT-DNA (200 μM) in the presence and absence of the complexes, respectively, were plotted against ratio (r) of [complex]/[DNA] ([complex]/[DNA] = 0.0–0.30) [28]. The viscosity values were calculated according to the relationship

$$\eta = (t - t^0)/t^0$$

where t and t_0 are the observed flow times in the presence and absence of the samples, respectively [29, 30].

Circular dichroism studies

CD spectra of CT-DNA (100 μM) were recorded in 5 mM Tris–HCl/50 mM NaCl buffer solution, pH 7.2 at room temperature by incrementing the [complex]/[CT-DNA] ratio (r = 0.0, 0.2, 0.4, 0.6, 0.8 and 1.0). The experiments were performed under a nitrogen atmosphere. The CD spectra were measured as the average of three independent scans from 220 to 320 nm.

Cyclic voltammetry

Cyclic voltammetric experiments were carried out with a CHI660C electrochemical workstation, purging the sample with N_2 prior to measurements. A standard three-electrode system comprising a Pt-microcylinder working electrode, a Pt-wire auxiliary electrode, and a saturated calomel reference electrode (SCE). The supporting electrolyte was comprised of 10 mM Tris–HCl/50 mM NaCl buffer solution (pH 7.2). The experiments were performed in 1.2 mM complex solutions in the absence and presence of CT-DNA.

DNA cleavage experiments

The cleavage of supercoiled pBR322 plasmid DNA (250 ng) was monitored using agarose gel electrophoresis. The sample was incubated for 1 h at 37 °C in the dark. A loading buffer was then added and electrophoresis performed at 100 V for 45 min in Tris–boric acid–EDTA (TBE) buffer (pH 8.3) using 0.8% agarose gel containing 5 mL GoldView. After electrophoresis, the bands were visualized under UV light and photographed using a Bio-Rad Laboratories-Segrate Gel Imaging System.

Molecular docking studies

The molecular docking studies were performed using the AutoDock 4.2 program [31] to investigate the interactions between the complex and DNA containing iodinated 12-mer oligonucleotides d(C-G-C-G-A-A-T-T-BrC-G-C-G)$_2$ (PDB ID: 6BNA). The B3LYP hybrid density functional was used to optimize the structure of the complex with the Gaussian 09 program package. The LanL2DZ basis set was used for Cu, and the 6-31G* basis set was used for other atoms. Before docking, water molecules and substrate were deleted, while polar hydrogen atoms and Gasteiger charges were added. The docking was performed in a 60 × 60 × 60 grid box with 0.375 Å spacing. A total of 100 runs of the Lamarckian genetic algorithm were performed. All other parameters were left at their default settings. All calculations

were carried out on a Dell T7500 server with dual XEON 5660 cores. The hydrogen bonds and visual results were handled using PyMol software (The PyMOL Molecular Visualization System, Version 1.5, Schrödinger, LLC).

In vitro cytotoxicity assays

In vitro cytotoxicity tests were carried out using the MTT assay [32]. Human tumor cell lines Eca-109, HeLa, A549, and human normal LO2 cells were seeded into 96-well microtiter plates (1×10^4 cells per well) and incubated overnight in a humidified atmosphere containing 5% CO_2 at 37 °C. The test complex was dissolved in DMSO and diluted with RPMI 1640 (10% fetal bovine serum (FBS), 100 units per mL penicillin and 50 units per mL streptomycin). The concentrations of the complex ranged from 1.57 to 100 μM. Control wells were prepared by the addition of culture medium (200 mL). The plates were incubated in a 5% CO_2 incubator at 37 °C for 48 h. A 10 μL aliquot of stock MTT dye solution (20 mL, 5 mg mL^{-1}) was then added to each well. After incubation at 37 °C for 4 h, buffer (100 mL) containing dimethylformamide (50%) and sodium dodecyl sulfate (20%) was added to transform MTT to a purple formazan dye. The optical density (OD) of each well was then measured at 595 nm on a microplate spectrophotometer.

Apoptosis studies

Eca-109 cells (2×10^5) were seeded onto chamber slides in six-well plates and incubated for 24 h. The cells were cultured in RPMI 1640 (10%, FBS) and incubated at 37 °C under a 5% CO_2. The medium was removed and replaced with fresh medium containing the complex (6.25 μM), then the plates were incubated for 24 h. The cells were washed with ice-cold PBS and fixed with formalin (4%, w/v). The cell nuclei were stained with AO/EB (100 mg mL^{-1} AO, 100 mg mL^{-1} EB) for 10 min, then imaged under a fluorescence microscope (Nikon, Yokohama, Japan) with excitation at 350 nm and emission at 460 nm.

Comet assays

DNA damage was investigated using the comet assay according to the literature procedure [5]. Briefly, Eca-109 cells in culture medium were incubated with 6.25 μM of the complex for 24 h at 37 °C. The cells were harvested by trypsinization after 24 h. A total of 100 μL of 0.5% normal agarose in PBS was dropped gently onto a fully frosted microslide, covered immediately with a coverslip, and then kept at 4 °C for 10 min. The coverslip was removed after the gel had set. A mixture of 50 μL of the cell suspension (200 cells/μL) mixed with 50 μL of 1% low-melting agarose was incubated at 37 °C. A total of 100 μL of this mixture was applied quickly on top of the gel, coated over the microslide, covered immediately with a coverslip, and then kept at 4 °C for 10 min. The coverslip was again removed after the gel had set. A third coating of 50 μL of 0.5% low-melting agarose was placed on the gel and kept for 15 min at 4 °C. After solidification of the agarose, the coverslips were removed, and the slides were immersed in an ice-cold lysis solution (2.5 M NaCl, 100 mM EDTA, 10 mM Tris, 90 mM sodium sarcosinate, NaOH, pH 10, 1% Triton X-100 and 10% DMSO) and kept at 4 °C for 2 h. All of the above operations were performed under low-lighting conditions to avoid additional DNA damage. Electrophoresis was then carried out at 25 V and 300 mA for 20 min. After electrophoresis, the cells were stained with 20 μL of EB (20 μg mL^{-1}) for 20 min in the dark. The slides were washed in chilled distilled water for 10 min to neutralize the excess alkali, air-dried and scored for comets by fluorescence microscopy.

Reactive oxygen species assays

2′,7′-Dichlorodihydrofluorescein diacetate (DCFH-DA) was used as a fluorescent probe to measure the ROS levels. Eca-109 cells were seeded into six-well plates (1×10^6 cells). After culturing for 24 h, the medium was replaced with fresh medium containing different concentrations of complex. The cells were then cultured 6 h, before staining with 20 μM DCFH-DA in PBS for 30 min in the dark. Finally, the cells were harvested and washed twice with PBS. The DCF fluorescence intensity was also determined.

Measurement of mitochondrial membrane potential

Eca-109 cells (2×10^5 per well) were treated with the complex for 24 h. JC-1 (1 mg/mL), which was used as a fluorescence probe to detect the changes of mitochondrial membrane potential, was added to stain the cells for 30 min at 37 °C. The cells were then washed twice with PBS and the fluorescence intensity of JC-1 was determined with a flow cytometer.

Intracellular Ca^{2+} levels

Eca-109 cells were treated with different concentrations of the complex for 24 h. The cells were incubated with 2.5 μM Fluo-3AM for 30 min at 37 °C, then the cells were washed three times and incubated for 20 min at 37 °C to ensure that Fluo-3AM had been completely transformed into Fluo-3. The cells were then washed twice with PBS and stained with 5 μg mL^{-1} DAPI solution. Finally, an ImageXpress Micro XLS system was used to observe fluorescence, and a multiwavelength cell scoring module was used to analyze the data. The fluorescence intensity per cell, which is

proportional to the level of Ca^{2+}, was calculated as the total fluorescence intensity divided by the number of cells.

Cytochrome *c* assays

Eca-109 cells were seeded in a 12-well plate and incubated overnight. The cells were treated with 3.13 or 6.25 μM of the complex for 24 h, and then fixed with ice-cold immunol staining fix solution for 30 min at room temperature. After blocking the cells with immunol staining blocking buffer for 1 h, the cells were treated with the primary antibody against cytochrome *c* (cyt-*c*, 1:50 dilution) overnight at 4 °C. Next, the plate was washed three times with immunol staining buffer and assayed with Alexa Fluor 488-Labeled Goat Anti-Mouse IgG (1:500 dilution) in the dark for 1 h at room temperature. Finally, the cells were washed three times with immunol staining wash buffer, and the cell nuclei were stained with DAPI. Images were obtained using an ImageXpress Micro XLS system, and the multiwavelength cell scoring module was used to analyze the data. The integrated intensity/cell representing the fluorescence intensity of each cell was used to measure the release of cyt-*c*. The fluorescence intensity per cell was calculated as the total fluorescence intensity divided by the number of cells.

Cell cycle arrest studies

Eca-109 cells (10^6 cells per well) were seeded into six-well plates (Costar, Corning Corp., New York, NY, USA) and cultured in RPMI 1640 (10% of FBS), by incubation at 37 °C and 5% CO_2. The medium was removed, and fresh medium (DMSO concentration 0.05% v/v) containing 6.25 μM of the complex was added to the cells. After incubation for 24 h, the cell layer was trypsinized, washed with cold PBS, and fixed with 70% ethanol. A 15-μL aliquot of RNAse (0.2 mg/mL) and 15 μL of propidium iodide (0.02 mg/mL) were added to the cell suspensions, which was then incubated for 30 min at 37 °C. The samples were analyzed with an FACS Calibur flow cytometry instrument.

Results and discussion

Synthesis and characterization

The complex [Cu(HPBM)(L-Phe)(H_2O)]·ClO_4 (**1**) was synthesized by the direct reaction of copper(II) perchlorate hexahydrate with HPBM and L-Phenylalanine in equimolar quantities using 80% methanol as solvent. The complex was purified by slow evaporation of solvent at room temperature. The molar conductivity of a 1 mM solution of the complex in methanol was 87.8 S cm^2 mol^{-1}, indicating that a 1:1 electrolyte in which the anion ClO_4^- is not coordinated. The UV–Vis spectra of HPBM (10 μM) and the complex (10 μM) were recorded in methanol. As shown in Fig. S1 (supporting information), a shift of 27 nm in the maximum absorption wavelength (300–400 nm) is observed for the complex compared with free HPBM. In addition, the complex (10 μM) was luminescent in methanol solution at ambient temperature, with the maximum appearing at 436 nm. The complex was also characterized by elemental analysis, IR, ESI–MS, and HR–ESIMS. The elemental analyses were in good agreement with the calculated values. In the assay of IR spectra of the complex **1**, a band at 3446 cm^{-1} is attributed to O–H stretching vibrations of H_2O, and a band at 3321 cm^{-1} is assigned to $–NH_2$ stretching vibrations. These data are comparable with those for [Cu(Gly-L-val)(HPB)(H_2O)]ClO_4 (O–H: 3420 cm^{-1}, N–H: 3322 cm^{-1}) [20]. No characteristic peak for –COOH (1700–1750 cm^{-1}) was observed, consistent with coordination of this group to the copper atom. Two peaks at 1589 and 1404 cm^{-1} are attributed to asymmetric ν_{as} ($-COO^-$) and symmetric ν_s ($-COO^-$) stretching frequencies. The frequency separation $\Delta\nu$ [$= \nu_{as}(-COO^-) - \nu_s(-COO^-)$] of 18 S cm^{-1} is consistent with unidentate coordination of the carboxylate group. In the ESI–MS and HR–ESIMS spectra of the complex, the observed molecular weight matched exactly with that of the coordination cation [Cu(HPBM)(L-Phe)]$^+$. The X-band ESR spectrum shows that $g_{\|} > g_{\perp}$ which indicates that the unpaired electron is located in the copper(II) d_{x2-y2} orbital, with an approximate square–pyramidal geometry. Additionally, according to Addison's parameter ($\tau = (\beta - \alpha)/60$), $\tau = 0.26$, which is also consistent with a square–pyramidal Cu(II) complex [33]. The distorted square–pyramidal structure was confirmed by single-crystal X-ray diffraction analysis. An ORTEP drawing of the cation is depicted in Fig. 1. Crystal data, selected bond lengths, and bond angles are collected in Tables 1 and 2. The structure consists of a

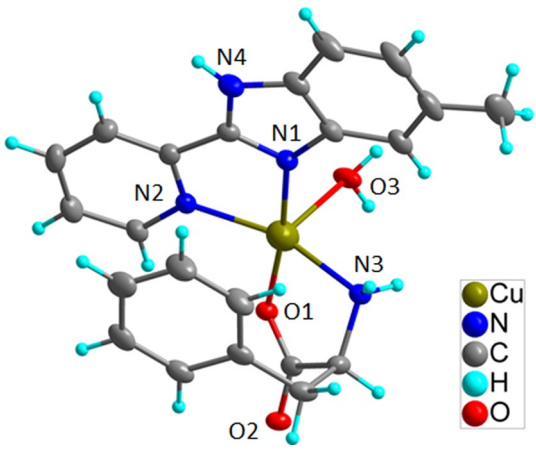

Fig. 1 An ORTEP drawing of the complex. The thermal ellipsoids probability level is 30%

Table 1 Selected crystallographic data for the complex

	$C_{22}H_{23}N_4O_7ClCu$		
Formula weight	552.43	Crystal size (mm^3)	0.21 × 0.19 × 0.16
Space group	Orthorhombic, P2(1)2(1)2(1)	Temp (K)	293 (2) K
a (Å)	10.9386(4)	θ range for data collection (°)	4.30–75.33
b (Å)	13.8994(3)	No. of data/parameters/restraints	6936/4316
c (Å)	15.3101(4)	Index ranges	$-12 \le h \le 13$, $-17 \le k \le 8$, $-14 \le l \le 19$
V ($Å^3$)	2327.75(12)	Goodness-of-fit on F2	1.050
Z	4	Final *R* indices [$I > 2\sigma(I)$]	$R_1 = 0.0418$, $wR_2 = 0.1106$
Dcalc (g cm^{-3})	1.582	*R* indices (all data)	$R_1 = 0.0442$, $wR_2 = 0.1141$
μ (Mo Kα) (mm^{-1})	2.839	Largest diff. peak and hole (e $Å^{-3}$)	0.586 and − 0.470
F (000)	1140		

Table 2 Selected bond lengths (Å) and angles (°) for complex

Bond length	(Å)	Bong angle	(°)
Cu(1)–O(1)	1.949(2)	O(1)–Cu(1)–N(1)	173.05(11)
Cu(1)–N(1)	1.975(3)	O(1)–Cu(1)–N(3)	81.91(11)
Cu(1)–N(2)	2.037(3)	N(1)–Cu(1)–N(3)	102.47(12)
Cu(1)–N(3)	2.023(3)	O(1)–Cu(1)–N(2)	92.90(10)
Cu(1)–O(3)	2.281(3)	N(1)–Cu(1)–N(2)	81.00(11)
		N(3)–Cu(1)–N(2)	157.53(11)
		O(1)–Cu(1)–O(3)	94.42(10)
		N(1)–Cu(1)–O(3)	90.78(11)
		N(3)–Cu(1)–O(3)	92.68(12)
		N(2)–Cu(1)–O(3)	109.56(11)

$[Cu(HPBM)(L\text{-}Phe)(H_2O)]^+$ cation and a ClO_4^- anion. The Cu(II) center of the complex is chelated by HPBM and an L-Phe ligands, and the axial position is occupied by a water ligand. The average Cu–N bond length is 2.011 (3) Å, which is smaller than that reported for $[Cu(glygly)(PyTA)]^+$ (2.014 (3) Å) [21].

DNA-binding studies

Electronic absorption titration

Electronic absorption spectroscopy is a useful method to determine the interactions of metal complexes with DNA. The electronic spectrum of the complex titrated with CT-DNA is shown in Fig. S2 (supporting information). As the concentration of DNA is increased, the metal-to-ligand charge transfer transition (MLCT) bands of the complex at 340 nm exhibits hypochromism of about 20.1%. These observations indicate that the complex interacts with DNA most likely through a mode that involves a stacking interaction between the aromatic chromophore and the base pairs of DNA. The DNA-binding constant of the complex was determined by monitoring the changes in the MLCT bands with increasing DNA concentration, giving a value of 7.38 (± 0.57) × 10^4 M^{-1}. This is smaller than that of [Cu(Gly-L-val)(HPB)(H_2O)]·ClO_4 (3.21 × 10^5 M^{-1}) [20], which may be due to steric hindrance from the methyl group of HPBM, and/or the different amino acid coordination.

Viscosity measurements

Viscosity measurements that are sensitive to the change in length of DNA are regarded as the least ambiguous and the most critical test of the binding mode in solution in the absence of crystal structure [30, 34]. In general, classical intercalation results in lengthening of the DNA helix, as the base pairs are separated to accommodate the binding ligand, leading to an increase in DNA viscosity. In contrast, a partial intercalation and/or minor groove binding of the ligand can bend (or kink) the DNA helix, reducing its effective length and hence its viscosity [29, 34]. The effects of the complex, together with those of ethidium bromide (EB) on the viscosity of rod-like DNA are shown in Fig. S3 (supporting information). It is well known that EB increases the relative specific viscosity, due to the lengthening of the DNA double helix by intercalation. However, with increasing the concentration of the present complex, the relative viscosity of DNA solution was decreased compared with that of the control. Hence, the results suggest that the complex interacts with DNA through a partial intercalative or minor groove binding mode.

Circular dichroism

Circular dichroism (CD) spectroscopy is a very sensitive technique, commonly used to monitor the possible conformational changes of DNA upon interaction with metal complexes. In general, CD spectra of DNA consist of two characteristic peaks (a positive band at 275 nm due to base

stacking and a negative band at 246 nm due to the right-handed helicity of B-DNA). As shown in Fig. S4 (supporting information), with increasing ratios of [Cu(II)/[DNA], the intensities of both the positive and negative bands decrease gradually (shifting to zero levels). The positive and negative peaks exhibit red shifts of 2 and 1 nm, respectively. These data indicate that the interaction of the Cu(II) complex with DNA disturbs the right-handed helicity and base stacking, inducing certain conformational changes in the B-DNA [35]. The small changes in the positive bands demonstrate that the complex intercalates partially into the DNA base pairs, and thereby unwinding the double helix [36, 37], which is consistent with the results obtained by viscosity measurements. Similar results have been observed in other Cu(II) complexes [20, 21].

Cyclic voltammetry

Cyclic voltammetry (CV) can afford useful information on the binding of metal complexes to DNA, because of the resemblance between electrochemical and biological reactions. It is well known that if a metal complex binds with DNA via electrostatic interactions, the electrochemical potential of the complex will shift in the negative direction. Conversely, intercalation to DNA results in a positive shift in potential. The electrochemical behavior of the complex was studied in methanol by CV in the absence or presence of CT-DNA. The CV of the complex exhibited one oxidation and one reduction peak in the sweep range from − 0.4 to 0.7 V, with a scan rate of 100 mv/s. As shown in Fig. S5 (supporting information), no new peaks were observed upon addition of CT-DNA to the complex, with R ([Cu(II)]/[DNA]) = 3. In the absence of CT-DNA, the $E_{1/2}$ value of Cu(I)/Cu(II) of the couple was 0.263 V, while in the presence of DNA (400 μM), the $E_{1/2}$ value was 0.319 V. Hence, an increase of 0.056 V in the $E_{1/2}$ value was observed, indicating that the complex interacts with CT-DNA through an intercalative or partially intercalative mode.

DNA cleavage studies

The cleavage of pBR322 DNA in the presence of the complex was investigated by agarose gel electrophoresis. In general, when circular plasmid DNA is subject to electrophoresis, relatively fast migration will be observed for the intact supercoiled form (Form I). If scission occurs on one strand (nicking), the supercoil will relax to generate a slower-moving open circular form (Form II). If both strands are cleaved, a linear form (Form III) that migrates between Form I and Form II will be generated [38]. The effect of the complex in the presence of Vitamin C (Vc) on pBR322 DNA (250 ng) is shown in Fig. S6 (supporting information). Evidently, for the control (lane 0, DNA alone), DNA + Vc (0.5 mM, lane 1) and the complex alone (10 μM, lane 2), no DNA cleavage was observed. However, in the presence of Vc, 5 (lane 3), 7.5 (lane 4) and 10 μM (lane 5) of the complex resulted in concentration-dependent DNA cleavage, such that the amount of Form I decreased gradually, whereas the amount of Form II increased. Thus, we infer that Vc acts as an initiator for the complex to cleave pBR322 DNA.

Molecular docking studies

Molecular docking calculation can be helpful for rational drug design and mechanistic studies, by placing a small molecule into the binding site of the DNA target region, mainly in a non-covalent mode [30]. Hence, to explore the interaction of the complex with B-DNA (PDB ID: 6BNA), the system was modeled with AutoDock 4.2 [31]. As shown in Fig. 2, we were able to obtain a model in which the complex interacted with DNA through a minor groove binding mode, in agreement with the results of the viscosity measurements. The resulting relative binding energy of the docked complex with DNA was − 40.15 kJ mol^{-1}. Figure 2 also shows that two hydrogen bonds between the complex and DNA bases. The lengths of these hydrogen bonds are 2.576 Å (H1···6BNA:DT-19:O3′) and 2.215 Å (O1···6BNA:DA-18:H3).

Cell viability assays by MTT method

The viabilities of cancer Eca-109, HeLa, A549, and normal LO2 cells in the presence of HPBM and the complex was investigated by the 3-(4,5-dimethylthiazole)-2,5-diphenyltetraazolium bromide (MTT) method. After incubation

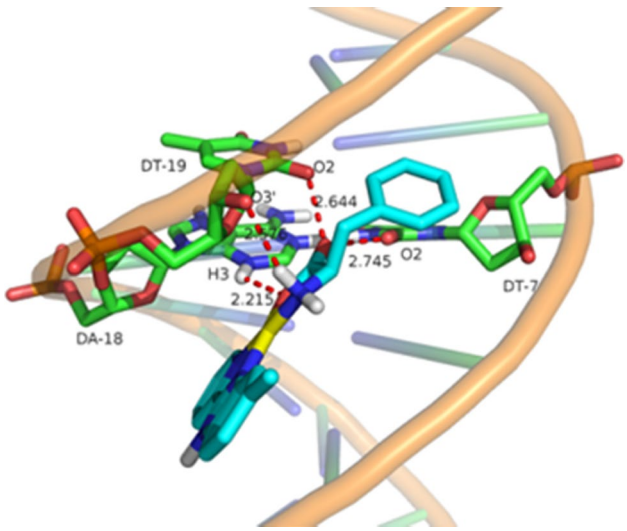

Fig. 2 The molecular docked models of the complexes with DNA. The hydrogen bonds between the complex and DNA are represented using red dashed lines. (Color figure online)

of the cells with different concentrations (1.57 → 100 μM) of the complex for 48 h, the viabilities in the presence of HPBM (a) and the complex (b) are depicted in Fig. S7 (supporting information), and the IC_{50} values are listed in Table 3. For free HPBM, when the concentration of HPBM reaches 100 μM, the cell viability is still more than 50%. The complex exhibits high cytotoxic activities toward Eca-109, HeLa, and A549 cells, with IC_{50} values of 5.7 ± 0.1, 8.3 ± 0.6, and 7.1 ± 0.5 μM, respectively. The cytotoxic activity of the complex against A549 cells is however lower than that of [Cu(Gly-L-val)(HPB)(H_2O)]ClO_4 (IC_{50} = 2.84 ± 0.19 μM) [20], but comparable with that of [Cu(dppt)$_2$(H_2O)](PF_6)$_2$ (dppt = 5,6-diphenyl-3-(2-pyridyl)-1,2,4-triazine) (IC_{50} = 7.80 ± 0.25 μM) [11]. Since Eca-109 cells were most sensitive to the complex, this cell line was selected to undergo the following biological activity tests.

Apoptosis studies

Apoptosis was assayed using the acridine orange (AO)/ethidium bromide (EB) double staining method. It is well known that AO can pass through cell membranes, but EB cannot. Hence, AO can stain the living and apoptotic cells green, while EB stains necrotic cells red. As shown in Fig. 3, in the control (a), living Eca-109 cells were stained bright green in spots and kept nuclei integrity. After Eca-109 cells were treated with 6.25 μM of the complex for 24 h (b), the apoptotic cells were bright green, with obvious apoptotic features such as nuclear shrinkage and chromatin condensation. These results suggest that the complex can induce apoptosis in Eca-7901 cells.

Table 3 The IC_{50} (μM) values of the Cu(II) complex and ligand HPBM toward the selected cell lines

Compound	Eca-109	HeLa	A549	LO2
HPBM	127.6 ± 3.3	102.6 ± 2.5	148.9 ± 7.6	111.5 ± 9.8
Cu(II) complex	5.7 ± 0.1	8.3 ± 0.6	7.1 ± 0.5	7.9 ± 0.7

Comet assays

Single cell gel electrophoresis (comet assay) in an agarose gel matrix was used to study DNA fragmentation, which is a hallmark of apoptosis [39]. As shown in Fig. 4, in the control experiments (a), the cells failed to show a comet-like appearance. When Eca-109 cells were treated with 3.13 or 6.25 μM of the complex (b and c) for 24 h, the cells displayed well-formed comets. The extent of DNA damage, which was estimated from the length of the comet tail, increased in a concentration-dependent manner. Hence, this complex can clearly induce DNA fragmentation, which will result in apoptosis.

Reactive oxygen species assay

A number of potential anticancer agents induce apoptosis through the generation of reactive oxygen species (ROS). 2′,7′-Dichlorodihydrofluorescein diacetate (DCFH-DA) was used as fluorescence probe to assay the cellular ROS levels induced by the complex. In the presence of intracellular esterases, DCHF-DA is transformed into a fluorescent product, namely, dichlorofluorescein (DCF). As shown in Fig. 5a, in the control experiment (a), no obvious fluorescent points were observed. After the treatment of SGC-7901 cells with either Rosup or the Cu(II) complex, a large number of green fluorescent points were found. The DCF fluorescence intensity was quantified with a multiwavelength cell scoring module; this is proportional to the amount of ROS produced by the cells. As shown in Fig. 5b, in the negative control, the DCF fluorescence

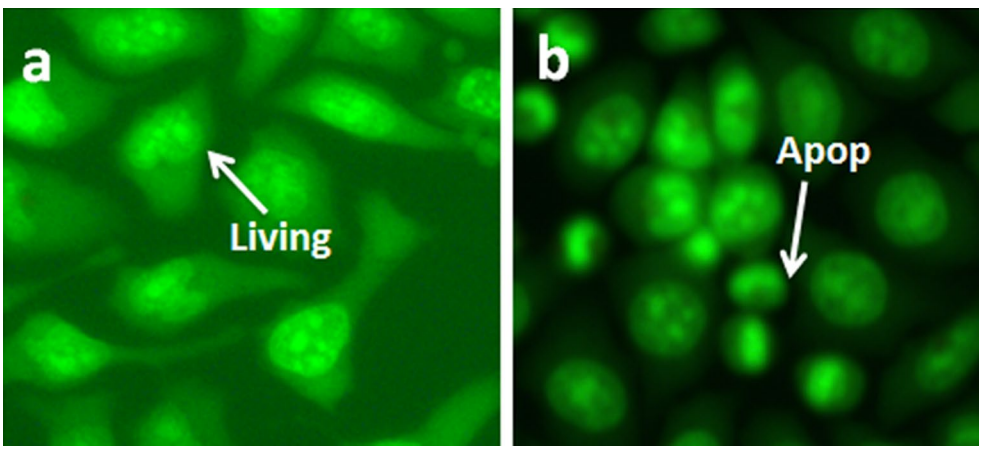

Fig. 3 Eca-109 (**a**) were exposed to 6.25 μM of the complex (**b**) for 24 h and stained with AO/EB and imaged under fluorescence microscope

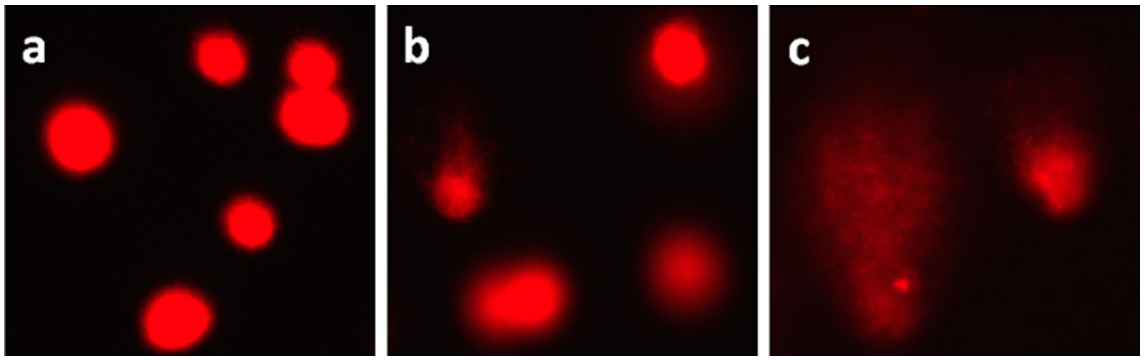

Fig. 4 Comet assay of EB-stained control (**a**) and 3.13 and 6.25 μM of the complex (**b**, **c**) treated Eca-109 cells at 24 h incubation

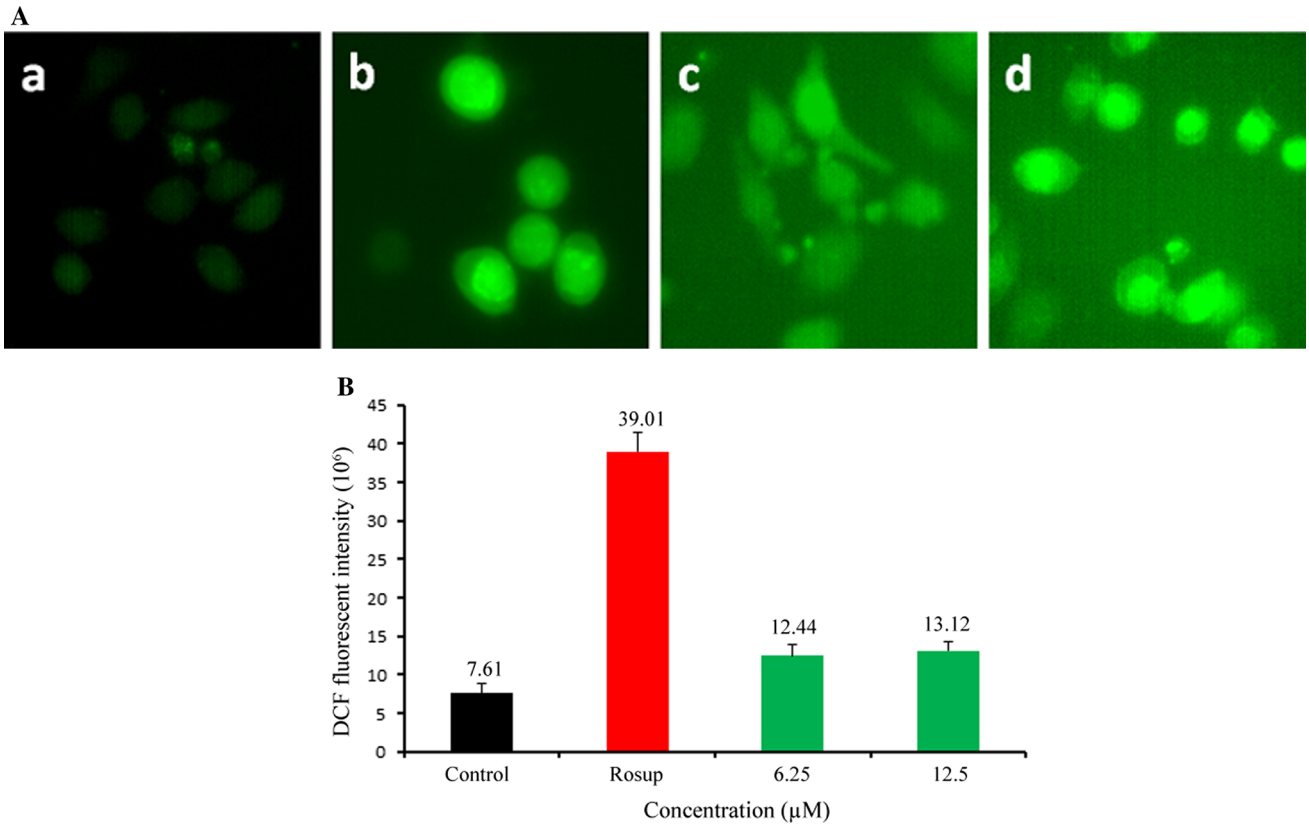

Fig. 5 **A** Intracellular ROS levels assay of Eca-109 cells (a) exposure to Rosup (b, positive control) and 6.25 (c) and 12.5 μM (d) of the complex for 6 h. **B** The DCF fluorescence intensity was determined in Eca-109 cells exposure to Rosup (50 μM, a positive control, 30 min) and 6.25 and 12.5 μM of the complex for 6 h

intensity was 7.61. When Eca-109 cells were incubated with either 6.25 or 12.5 μM of the complex for 6 h, the DCF fluorescence intensity was increased in a concentration-dependent manner. These results indicate that the complex can increase intracellular ROS levels.

Mitochondrial membrane potential

Mitochondria play an important role in apoptosis through the release of pro-apoptotic factors, including cytochrome *c* and the apoptosis-inducing factor [40, 41]. The changes

of mitochondrial membrane potential (MMP) in Eca-109 cells treated the complex were investigated using JC-1 as fluorescent probe. JC-1 emits red fluorescence at high MMP, while at low MMP, JC-1 emits green fluorescence. The ratio of red/green fluorescence intensity was determined by flow cytometry. As shown in Fig. 6, in the control (a, up and down), the ratio of red/green was 4.17. When Eca-109 cells were treated with carbonylcyanide-m-chlorophenylhydrazone (cccp), 6.25 or 12.5 μM of the complex for 24 h, the ratio of red/green fluorescence decreased. Hence, the complex can induce a concentration-dependent decrease in the mitochondrial membrane potential.

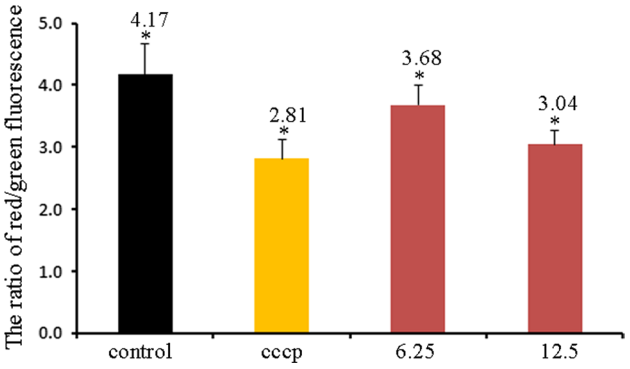

Fig. 6 Assay of Eca-109 cells mitochondrial membrane potential with JC-1 as fluorescence probe staining method. The ratio of red/green fluorescence after Eca-109 cells exposed to cccp (positive control) and 6.25 and 12.5 μM of the complex for 24 h

Intracellular calcium levels

High intracellular levels of Ca^{2+} are associated with the induction of cell death. [42]. The intracellular Ca^{2+} levels in the presence of the complex were therefore assayed using Fluo-3AM (indicating cytosolic Ca^{2+}) as a fluorescent probe, which combines with Ca^{2+} to give Fluo-3. The intracellular Ca^{2+} level in Eca-109 cells induced by the complex was determined using on ImageXpress Micro XLS system and multiwavelength cell scoring module. As shown in Fig. 7a, in the control experiment (a), no obvious green fluorescent points were observed, consistent with a very low level of

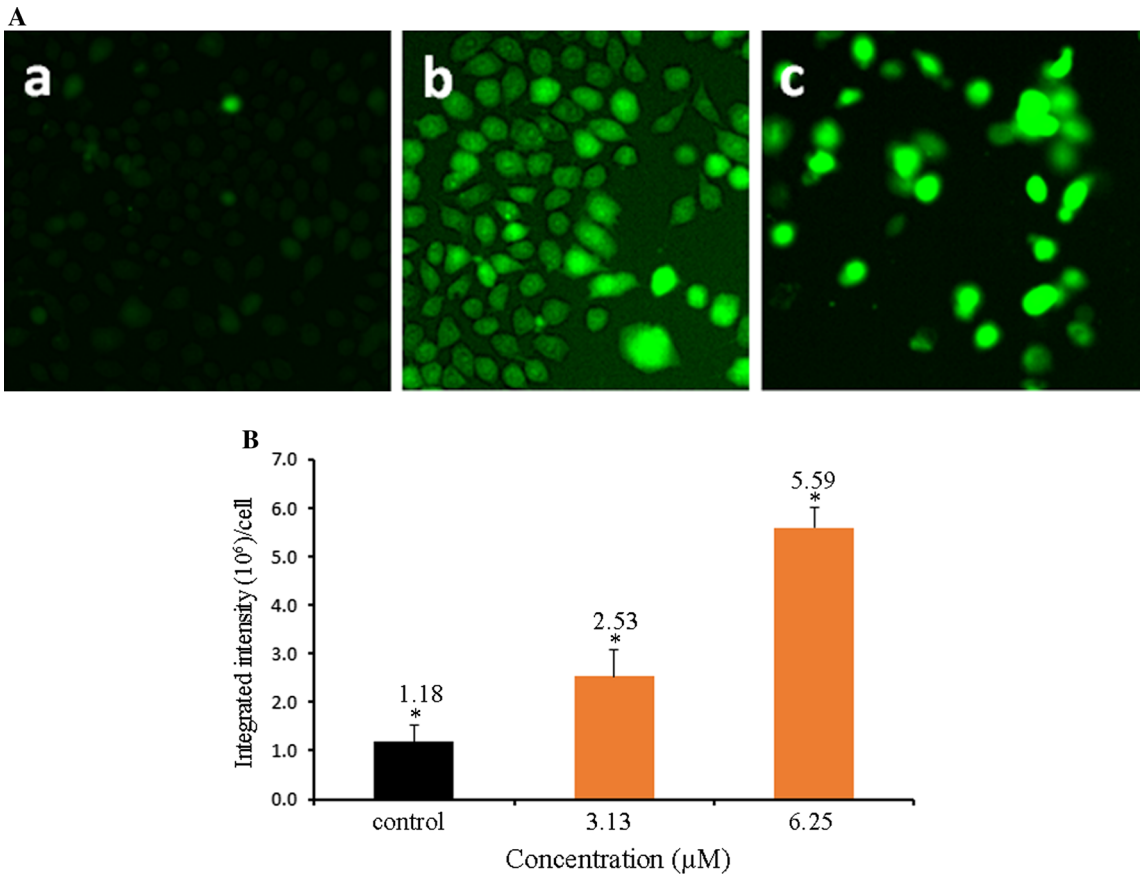

Fig. 7 **A** Intracellular Ca^{2+} levels were assayed after Eca-109 cells were exposed to 3.13 and 6.25 μM of the complex for 24 h. **B** The integrated fluorescent intensity/cell was determined after Eca-109 cells were treated with different concentration of the complex for 24 h. *$P < 0.05$ represents significant differences compared with control

intracellular free Ca^{2+}. After treatment of the Eca-109 cells with different concentrations of the complex (b and c) for 24 h, a number of bright green fluorescence points were observed, indicating that the complex can increase intracellular Ca^{2+} levels. To quantitatively determine this effect, the fluorescence intensity of Flu-3 was determined as shown in Fig. 7b. The results demonstrate that the complex can enhance the level of intracellular Ca^{2+} in a dose-dependent manner, which further increases intracellular ROS levels.

Cytochrome *c* assays

Cytochrome *c* (cyt-*c*) can induce cell apoptosis by activating caspase proteases, which are released from the mitochondrial membrane space under conditions of mitochondrial dysfunction [43]. The high concentration of intracellular Ca^{2+} and reduction in MMP may lead to the release of cytochrome *c* from the mitochondria. As shown in Fig. 8a, in the control experiment, no obvious green fluorescent points

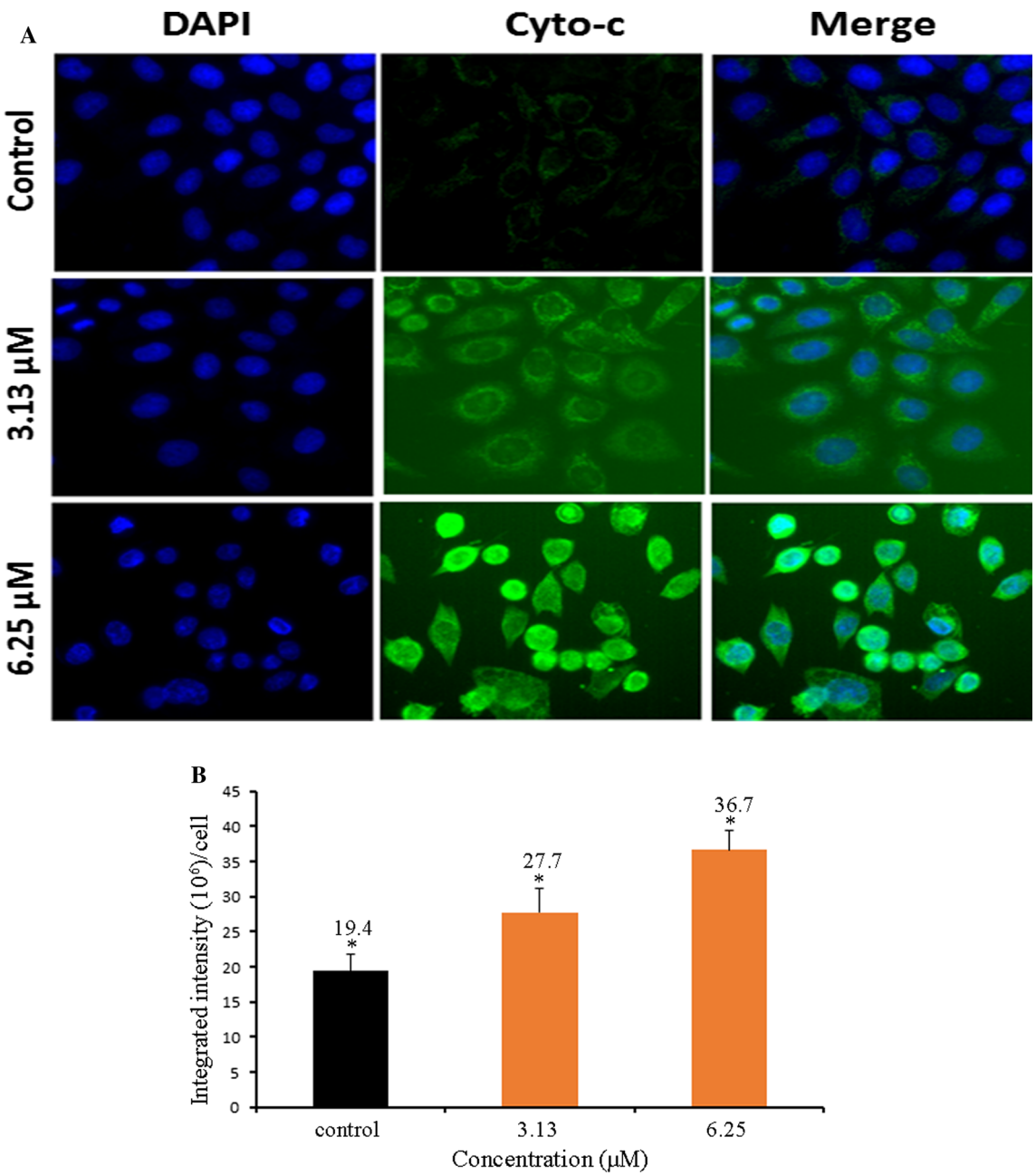

Fig. 8 **A** The release of cyt-*c* was examined after Eca-109 cells were exposed to different concentration of the complex for 24 h. **B** The integrated fluorescent intensity/cell was determined after different concentration of the complex treated Eca-109 cells for 24 h. *$P < 0.05$ represents significant differences compared with control

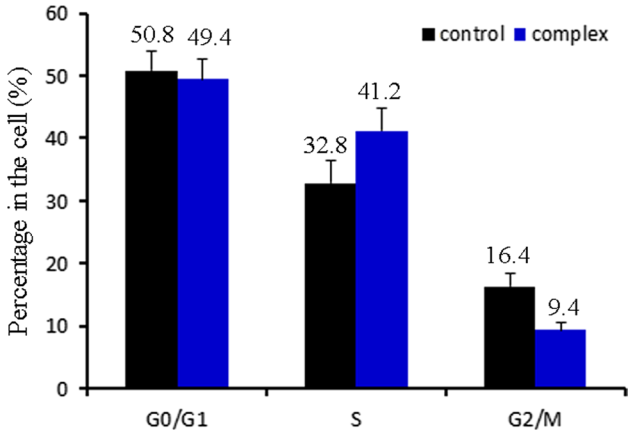

Fig. 9 Cell cycle distribution of Eca-109 cells exposure to 6.25 μM of the complex for 24 h

were observed. Upon incubation of Eca-109 cells with 3.13 or 6.25 μM of the complex for 24 h, green fluorescent points were observed, consistent with a release of cyt-*c*. As shown in Fig. 8b, with increasing concentrations of the complex, the integrated fluorescence intensity increases. Hence, the complex shows a concentration-dependent release of cyt-*c*.

Cell cycle arrest studies

Inhibition of cancer cell proliferation by cytotoxic drugs can result from either induction of apoptosis, cell cycle arrest or a combination of both. The effect of the complex on the Eca-109 cell cycle was investigated using fluorescence-activated cell sorting (FACS) analysis of the DNA content. The cell cycle progression was analyzed at a 6.25 μM concentration of the complex for 24 h. As shown in Fig. 9, in the control experiment, the proportion of cells at S phase is 32.8%. Upon exposure of the cells to the complex, the proportion at S phase increases to 41.2%, accompanied by a corresponding reduction of 7.0% in the cells at G2/M phase. Hence, the complex induces cell cycle arrest at S phase.

Conclusions

A copper(II) complex of an aromatic heterocycle with an amino acid co-ligand was synthesized and characterized. DNA-binding studies indicate that the complex interacts with CT-DNA through a minor groove binding mode. The complex can induce apoptosis and DNA damage in Eca-109 cells. This is accompanied by an increase in ROS levels, plus a decrease in the mitochondrial membrane potential. In addition, the complex increases the intracellular Ca^{2+} levels and induces a release of cytochrome *c*. Cell cycle distribution studies reveal that the complex inhibits cell growth at the S phase. This work should pave valuable for the design and synthesis of new copper(II) complexes as potent anticancer drugs.

Acknowledgements We acknowledge the Program of Natural Science Foundation of Guangdong Province (2015A030313423) and Guangdong Province College Students' Innovation and Entrepreneurship Training Program (201710564307) for financial support.

References

1. Huang Z (2005) Technol Cancer Res Treat 4:283–293
2. Boulikas T, Vougiouka M (2003) Oncol Rep 10:1663–1682
3. Wong E, Giandomenico CM (1999) Chem Rev 99:2451–2466
4. Jamieson ER, Lippard SJ (1999) Chem Rev 99:2467–2498
5. Lai SH, Li W, Wang XZ, Zhang C, Zeng CC, Tang B, Wan D, Liu YJ (2016) RSC Adv 6:63143–63155
6. Alizadeh R, Yousuf I, Afzal M, Srivastav S, Srikrishna S, Arjmand F (2015) J Photochem Photobiol B Biol 143:61–73
7. Yousuf I, Arjmand F (2016) J Photochem Photobiol B Biol 164:83–95
8. Cui HL, Goddard R, Pörschke KR, Hamacher A, Kassack MU (2016) Inorg Chem 55:2986–2997
9. Asatkar AK, Tripathi M, Panda S, Pande R, Zade SS (2017) Spectrochim Acta Part A 171:18–24
10. Hasan MA, Kumari N, Singh K, Singh K, Mishra L (2016) Spectrochim Acta Part A 152:208–217
11. Anjomshoa M, Hadadzadeh H, Torkzadeh-Mahani M, Fatemi SJ, Adeli-Sardou M, Rudbari HA, Nardo VM (2015) Eur J Med Chem 96:66–82
12. Kaim W, Rall J (1996) Angew Chem Int Ed 35:43–60
13. Borthakur R, Kumar A, Lemtur A, Lal RA (2013) RSC Adv 3:15139–15147
14. Marzano C, Pellei M, Tisato F, Santini C (2009) Anti-Cancer Agents Med Chem 9:185–211
15. Sigel A, Sigel H (eds) (1996) Metal ions in biological systems, vol 33. Marcel Dekker, New York, p 177
16. Ji LN, Zou XH, Liu JG (2001) Coord Chem Rev 216–217:513–536
17. Vaidyananthan VG, Nair BH (2005) Dalton Trans 17:2842–2848
18. Maheswari PU, Palaniandavar M (2004) Inorg Chim Acta 357:901–912
19. Santini C, Pellei M, Gandin V, Porchia M, Tisato F, Marzano C (2014) Chem Rev 114:815–862
20. Gan Q, Zhang CL, Wang BF, Xiong YH, Fu YL, Mao ZW, Le XY (2016) RSC Adv 6:35952–35965
21. Fu XB, Liu DD, Lin Y, Hu W, Mao ZW, Le XY (2014) Dalton Trans 43:8721–8737
22. Marmur J (1961) J Mol Biol 3:208–218
23. Reichmann ME, Rice SA, Thomas CA, Doty P (1954) J Am Chem Soc 76:3047–3053
24. Schiffmann R, Neugebauer A, Klein CD (2006) J Med Chem 49:511–522
25. Sheldrick GM (1996) SADABS, program for empirical absorption correction of area detector data. University of Gçttingen, Germany
26. Sheldrick GM (1997) SHELXL-97, program for crystal structure refinement. University of Gçttingen, Germany
27. Wolf A, Shimer GH Jr, Meehan T (1987) Biochemistry 26:6392–6396
28. Cohen G, Eisenberg H (1969) Biopolymers 8:45–55
29. Satyanaryana S, Daborusak JC, Chaires JB (1993) Biochemistry 32:2573–2584
30. Rohs R, Bloch I, Sklenar H, Shekked Z (2005) Nucleic Acids Res 33:7048–7057

31. Morris GM, Huey R, William W, Sanner MF, Belew RK, Goodsell DS, Olson AJ (2009) J Comput Chem 30:2785–2791
32. Mosmann T (1983) J Immunol Methods 65:55–63
33. Addison AW, Rao TN, Reedijk J, Rijn JV, Verschoor GC (1984) J Chem Soc Dalton Trans 7:1349–1356
34. Satyanarayana S, Dabroniak JC, Chaires JB (1992) Biochemistry 31:9319–9324
35. Mahadevan S, Palaniandavar M (1978) Inorg Chem 37:693–700
36. Xu XY, Wang DD, Sun XJ, Zeng SY, Li LW, Sun DZ (2009) Thermochim Acta 493:30–36
37. Li GY, Du KJ, Wang JQ, Liang JW, Kou JF, Hou XJ, Ji LN, Chao H (2013) J Inorg Biochem 119:43–53
38. Barton JK, Raphael AL (1984) J Am Chem Soc 106:2466–2468
39. Alapetite C, Wachter T, Sage E, Moustacchi E (1996) Int J Radiat Biol 69:359–369
40. Chilin A, Dodoni G, Frezza C, Guiotto A, Barbieri V, Lisa FD, Canton M (2005) J Med Chem 48:192–199
41. Miura T, Tanno M, Sato T (2010) Cardiovasc Res 88:7–15
42. Berridge MJ, Bootman MD, Roderick HL (2003) Nat Rev Mol Cell Biol 4:517–529
43. Liu X, Kim CN, Yang J, Jemmerson R, Wang X (1996) Cell 86:147–157